sustainability

IMPACT FACTOR 3.3

CITESCORE 7.7

Article

Dry Pass, Wet Fail: Ground Impedance Testing of Field-Aged PV Modules—Implications for Repowering/Revamping Within 5–10 Years and for Environmental Sustainability

Vladislav Poulek, Vaclav Beranek, Tomas Finsterle and Martin Kozelka

MDPI

https://doi.org/10.3390/su18031212

sustainability

MDPI

Article

Dry Pass, Wet Fail: Ground Impedance Testing of Field-Aged PV Modules—Implications for Repowering/Revamping Within 5–10 Years and for Environmental Sustainability

Vladislav Poulek [1,*], Vaclav Beranek [2], Tomas Finsterle [3] and Martin Kozelka [2]

[1] Faculty of Environmental Sciences, Czech University of Life Sciences, 16500 Prague, Czech Republic
[2] Faculty of Engineering, Czech University of Life Sciences, 16500 Prague, Czech Republic
[3] Faculty of Electrical Engineering, Czech Technical University in Prague, 16000 Prague, Czech Republic
* Correspondence: poulek@solar-solar.com

Abstract

The ground impedance (insulation resistance R_{isol}) of photovoltaic (PV) modules is usually measured only in the dry state, even though arrays frequently operate under dew-wet or rain-wet conditions, when leakage paths can change. We measured dry insulation resistance R_{dry} and IEC 61215 MQT 15 wet leakage resistance R_{wet} for N = 37 field-aged crystalline-silicon modules from utility-scale plants and related the results to the IEC 40 MΩ·m^2 criterion ($R_{wet} \times A \geq 40$). The measurements used 1000 V DC and a 2 min dwell; R_{wet} was obtained in a salted bath with a solution resistivity < 3500 Ω·cm. The median R_{dry} was 42.4 GΩ, whereas the median R_{wet} was 462.5 MΩ, resulting in a median R_{dry}/R_{wet} ratio of ~110×. Three modules (8.1%) failed the 40 MΩ·m^2 limit already in the dry state, whereas eight modules (21.6%) failed under IEC-wet conditions; five were dry-pass/wet-fail cases that would have passed dry screening. For a representative area A = 1.8 m^2, a practical conservative dry triage threshold of approximately 55.5 GΩ identifies modules needing IEC-wet verification rather than serving as a stand-alone limit. Overall, combining dry and IEC-wet measurements improves safety and supports sustainability through resource-efficient repowering/revamping and end-of-life decisions in large PV fleets, particularly in hot climates.

Keywords: photovoltaics; insulation resistance/ground impedance; IEC 61215; MQT 15; wet leakage; dew; repowering/revamping; reliability; sustainability

Academic Editor: Carlos Vargas-Salgado

Received: 17 December 2025
Revised: 18 January 2026
Accepted: 23 January 2026
Published: 25 January 2026

1. Introduction

The long-term safety and reliability of photovoltaic (PV) modules are essential for the performance and sustainability of large-scale PV installations. A key parameter in this context is the insulation resistance R_{isol} between the DC circuits and accessible conductive parts or ground. If R_{isol} becomes too low, leakage currents increase, ground-fault detection may trigger frequent trips, and in extreme cases, safety hazards for personnel and the public can arise. In routine practice, R_{isol} is usually assessed only in the dry state with an ohmmeter at several hundred volts to 1000 V DC, and the measured values are compared with acceptance criteria derived from IEC 61215, often expressed as a minimum resistance or a resistance–area product [1].

However, real PV modules in the field frequently operate under dew-wet, fog-wet or rain-wet conditions, especially in the early morning, when radiative cooling causes the front glass to fall below the ambient temperature and the dew point. Such dew-wet conditions

are common across climates and are not limited to desert environments [2]. Under such conditions, leakage paths along the glass surface, frame, edges, junction box and backsheet can differ substantially from those under dry conditions, and wet insulation resistance can be far lower than dry values [3–6]. The IEC 61215 MQT 15 wet leakage current test was designed to represent these wet operating conditions. In this test, a module is immersed in a conductive solution and biased at DC voltage; for modules larger than 0.1 m^2, the product $R_{wet} \times A$ must be at least 40 MΩ·m^2 to pass [1]. In practice, MQT 15 is primarily used for design qualification and type approval of new module designs [1,7]. Systematic IEC-conforming wet testing on larger sets of field-aged modules is therefore uncommon in routine O&M, where dry tests are often preferred owing to field time constraints [7].

Several studies have examined how insulation resistance depends on humidity, temperature and system voltage. Hernández et al. [3] linked array insulation resistance to environmental conditions and string voltage, showing that water ingress and surface wetting can significantly reduce R_{isol} at typical operating voltages. Roy [4] presented an equivalent-circuit model supported by dry and wet insulation measurements on a framed glass/EVA/Tedlar PV module of approximately 1.4 m^2 tested in an outdoor/immersion setup (with two wet configurations, front-side immersion and front + back immersion, while keeping the junction box out of water), but without reporting field service age (years in operation), specific operating climate/location, or module-to-module statistics (sample size not stated), unlike our IEC-MQT15 testing of N = 37 field-aged crystalline-silicon modules from utility-scale plants in Slovakia. Roy [4] modeled leakage through encapsulant–backsheet stacks, highlighting the role of water uptake, ion transport and the Arrhenius-type temperature dependence. Roy [4] also reported IEC-style dry and wet insulation measurements versus temperature. Two wet configurations are considered: front-side immersion only and front-plus-back immersion (with the junction box kept out of the water). The authors do not report module-to-module statistics (the sample size is not stated), as the experimental data mainly support the model rather than a statistical screening of field-aged modules [4]. Buerhop et al. [5] studied the development of wet leakage resistance for different backsheet types and demonstrated that some fluoropolymer-free backsheet constructions exhibit pronounced decreases in wet resistance with field exposure, leading to ground-impedance issues at inverters. Ketjoy et al. [6] investigated flooded PV modules and confirmed the strong impact of moisture pathways on wet leakage behavior. Backsheet-related insulation issues in multi-megawatt plants and their spectroscopic identification have been described in further detail in [8–10].

Beyond immediate safety, wet insulation resistance has implications for circularity and end-of-life strategies. Environmentally sustainable methods for recycling PV panels laminated with soft polysiloxane gels have been demonstrated, enabling mechanical delamination without burning or aggressive chemicals [11]. Other works have analyzed PV panel and inverter damage due to water penetration [12] and examined the effects of backsheet repairs on insulation resistance [13]. Broader reviews addressing PV end-of-life management and recycling from a sustainability perspective, including economic and process-related aspects, are provided in [14–17]. Together, these developments highlight the need to characterize insulation behavior under realistic wet conditions as part of a sustainable strategy for PV asset management.

At the same time, global PV deployment is increasingly concentrated in high-irradiance regions with very low levelized cost of electricity (LCOE), where partial repowering/revamping—replacement of older or underperforming modules with newer technology after 5–10 years—can be economically attractive [18–22]. In the following, we use the term repowering in a broad sense that also covers “revamping” concepts in which only part of the installed capacity is renewed while much of the existing infrastructure

remains in place. In such markets, reliable insulation-resistance data under realistic wet conditions are relevant not only for immediate safety but also for asset-management and the end-of-life decisions: whether modules can be kept in service, should be replaced in repowering campaigns, or directed to advanced recycling routes [11,14–17].

Accordingly, dry/wet ground impedance comparisons on statistically meaningful sets of field-aged modules and their interpretation in the context of routine morning-dew wetting remain limited—motivating the present study [2,7]. In this work, we address these questions by systematically comparing dry and IEC-wet insulation resistance for a set of field-aged crystalline-silicon modules.

- We quantify the relationship between dry (R_{dry}) and IEC-wet (R_{wet}) ground impedance (insulation resistance) for N = 37 field-aged modules;
- We document the occurrence of dry-pass/wet-fail modules that meet dry criteria but fail the IEC 40 MΩ·m^2 wet criterion;
- We derive a dry-test threshold that can serve as a conservative screening indicator for potential IEC-wet failure;
- How dry and wet insulation measurements can support safer operation, repowering/revamping, and contributing to sustainable PV fleet management and sustainability-oriented end-of-life strategies should be discussed.

2. Materials and Methods

2.1. Samples

We analyzed N = 37 field-aged crystalline-silicon PV modules originating from utility-scale plants operating in a very moderate Central European climate (Slovakia). To preserve the anonymity of suppliers and sites, module types are denoted by internal IDs. For each module, we recorded

- Module ID (internal);
- Wet insulation resistance R_{wet} with units (kΩ, MΩ, GΩ or catastrophic 0 Ω);
- Dry insulation resistance R_{dry} with units;
- Ratio R_{dry}/R_{wet} (dimensionless).

Modules with $R_{wet} \approx 0$ Ω are treated as catastrophic wet failures (“Cat.”). For these modules, the ratio R_{dry}/R_{wet} is not defined and they are handled as a separate category in the statistics. The full dataset is given in Table 1.

Table 1. Dry and IEC-wet insulation resistance of the 37 field-aged PV modules and dry-to-wet ratio. Units: k = kΩ, M = MΩ, G = GΩ. “Cat.” indicates catastrophic wet failure (R_{wet} below instrument range, reported as ~0 Ω); R_{dry}/R_{wet} is not defined for these modules.

Panel No.	R_{wet}	Unit (Wet)	R_{dry}	Unit (Dry)	Ratio R_{dry}/R_{wet}
1	1828	M	42.3	G	23.14
2	356	M	24.9	G	69.94
3	1051	M	21.5	G	20.46
4	183.4	M	36.7	G	200.11
5	216	M	53.7	G	248.61
6	1158	M	54.2	G	46.80
7	5.99	G	68.7	G	11.47
8	1658	M	61.1	G	36.85
9	1405	M	75.6	G	53.81
10	12.58	M	9.87	M	0.78

Table 1. *Cont.*

Panel No.	R_{wet}	Unit (Wet)	R_{dry}	Unit (Dry)	Ratio R_{dry}/R_{wet}
11	0	Ω	3.3	M	Cat.
12	49.5	M	42.4	G	856.57
13	1365	M	55.5	G	40.66
14	977	k	3.27	M	3.35
15	0	Ω	110.4	G	Cat.
16	0	Ω	29.5	G	Cat.
17	504	M	60	G	119.05
18	332	M	50.9	G	153.31
19	537	M	110	G	204.84
20	647	M	48.3	G	74.65
21	495	M	72.8	G	147.07
22	0	Ω	52.3	G	Cat.
23	157.4	M	35.2	G	223.63
24	175.4	M	21.9	G	124.86
25	139.4	M	42.1	G	302.01
26	142.3	M	23.9	G	167.96
27	120.2	M	18.08	G	150.42
28	0	Ω	103.5	G	Cat.
29	300	M	70.8	G	236.00
30	471	M	41.7	G	88.54
31	454	M	45.6	G	100.44
32	610	M	50.8	G	83.28
33	349	M	23.1	M	0.07
34	4.38	M	54.9	M	12.53
35	1435	M	42.3	G	29.48
36	594	M	35	G	58.92
37	290	M	37.6	G	129.66

2.2. Dry Insulation Resistance Measurements

The dry insulation resistance R_{dry} was measured at 1000 V DC using a calibrated insulation tester. Measurements were performed under ambient laboratory conditions (22 ± 2 °C, relative humidity 40–60%), and the modules were electrically isolated from the ground except through the tester.

For each module, the positive terminal of the tester was connected to the interconnected string of cells (short-circuited together), whereas the negative terminal was connected to the aluminum frame. After ramping to 1000 V, the voltage was held for a dwell time of 2 min, and the insulation resistance was then recorded.

For comparison with the IEC criteria, we computed the resistance–area product $R_{dry} \times A$ and compared it with 40 MΩ·m^2 for typical module areas A = 1.6–2.0 m^2. In practical applications, the exact module area should be used [1].

2.3. IEC 61215 MQT 15 Wet Leakage Test

The wet insulation resistance R_{wet} was measured following the MQT 15 wet leakage current test in IEC 61215 [1]. The test setup is illustrated schematically in Figure 1, and a photograph of the laboratory installation is shown in Figure 2. A non-conductive polypropylene (PP) tank equipped with a stainless-steel mesh electrode was filled with saltwater such that the solution resistivity remained below 3500 Ω·cm. The laboratory temperature was maintained at 22 ± 2 °C.

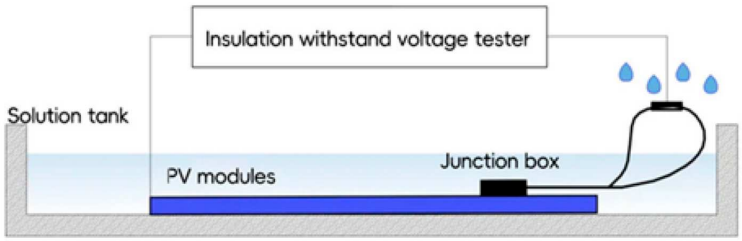

Figure 1. Schematic diagram of the measurement circuit (adapted from Firman et al. [23]).

Figure 2. Photograph of the actual laboratory installation with the PP tank, immersed module and insulation tester.

Each module was placed horizontally and immersed so that the front glass and frame were fully in contact with the solution; the junction box and cables were also wetted with the same solution by spraying. The module's output leads were short-circuited and connected to the positive terminal of the insulation tester, whereas the negative terminal was connected to the bath electrode. A DC voltage of 1000 V was applied, and after a 2 min dwell time, the insulation resistance R_{wet} was recorded. After each test, the module was discharged by briefly short-circuiting the leads to the frame.

For modules with areas $A > 0.1$ m^2, the IEC acceptance criterion is shown in Equation (1):

$$R_{\text{wet}} \times A \geq 40\ \text{M}\Omega\cdot\text{m}^2 \quad (1)$$

Equivalently,

$$R_{\text{wet}} \geq \frac{40}{A}\text{M}\Omega$$

where is R_{wet} the measured wet insulation resistance and A is the module area. This resistance–area product normalizes the acceptance criterion to module size. For representative module areas A = 1.6, 1.8, 2.0 m^2, the corresponding wet-resistance limits are R_{limit} = 25.0, 22.2, 20.0 MΩ, respectively. At V = 1000 V DC, these limits correspond to leakage currents $I_{leak} = V/R_{limit}$ on the order of 40–50 μA.

In this study, a representative area A = 1.8 m^2 is used to derive illustrative thresholds; in real applications, the actual module area should be used.

2.4. Data Analysis and Dry-Test Threshold

For each module, we computed the ratio:

Equation (2):

$$R_{\text{ratio}} = \frac{R_{\text{dry}}}{R_{\text{wet}}}, \tag{2}$$

(using consistent units, MΩ). Modules with $R_{wet} \approx 0$ are treated as catastrophic wet failures; R_{ratio} is not defined for these modules and they are handled as a separate category.

We also classified each module as passing or failing with respect to the IEC 40 MΩ·m^2 criterion for assumed areas A = 1.6, 1.8 and 2.0 m^2.

To derive a practical dry-test threshold usable as a simple screening rule, we considered A = 1.8 m^2 and scanned candidate thresholds T on R_{dry}. For each threshold, modules with $R_{dry} < T$ were flagged as "at risk", and we computed sensitivity and specificity:

Equation (3):

$$Sensitivity = \frac{TP}{TP + FN} \tag{3}$$

Equation (4):

$$Specificity = \frac{TN}{TN + FP} \tag{4}$$

where TP is the number of IEC-wet-failing modules correctly flagged as at risk, FN is the number of IEC-wet-failing modules missed by the dry threshold, TN is the number of IEC-wet-passing modules correctly not flagged, and FP is the number of IEC-wet-passing modules incorrectly flagged as at risk.

3. Results

3.1. Dry Versus IEC-Wet Insulation Resistance and Ratio Distributions

Across the N = 37 modules, the median wet insulation resistance R_{wet} was 462.5 MΩ, whereas the median dry resistance R_{dry} was 42.4 GΩ. Thus, at the median, the dry measurement overestimates the wet resistance by a factor of approximately 110. The median ratio R_{dry}/R_{wet} was 109.7×, with a mean ratio of 543.5×, indicating a strongly skewed distribution with a long tail toward very large dry–wet drops. Several modules exhibit ratios above 200, and five modules (Panels 11, 15, 16, 22 and 28) show catastrophic wet behavior with $R_{\text{wet}} \approx 0$ Ω, i.e., complete loss of insulation under wet conditions.

To visualize the modulewise behavior of the dry and IEC-wet insulation resistance, Figure 3 shows the R_{dry} and R_{wet} values for each module on a logarithmic MΩ scale. The modules with finite R_{wet} values are sorted along the x-axis by increasing the IEC-wet resistance, and the corresponding dry resistance is shown for the same modules. For every module in the plot, R_{dry} clearly exceeds R_{wet}, typically by one to two orders of magnitude, confirming that dry measurements systematically overestimate the insulation level that is relevant under wet operating conditions. Two modules (Panels 10 and 33) show $R_{dry} < R_{wet}$ (ratio < 1), which can occur due to measurement variability or transient surface/contact conditions. The lowest R_{wet} values cluster well below 100 MΩ, whereas most R_{dry} values remain in the 10^4–10^5 MΩ range. Modules with $R_{wet} \approx 0$ Ω cannot be shown on the logarithmic axis and are therefore omitted from Figure 3 but are included in the statistical analysis.

To summarize the ratio R_{dry}/R_{wet} in an intuitive way and explicitly include the modules with R_{wet} = 0 Ω, the ratios were grouped into five categories: Cat (R_{wet} = 0 Ω), 0–1, 1–10, 10–100 and 100–1000. The resulting categorical histogram is shown in Figure 4. Five modules fall into the "Cat." bin, two modules fall into the 0–1 bin ($R_{dry} < R_{wet}$), one module falls into the 1–10 bin, and fourteen and fifteen modules fall into the 10–100 and 100–1000 bins, respectively. Thus, most modules exhibit dry-to-wet drops exceeding one

order of magnitude, and many exceed two orders of magnitude. This skewed distribution underlies the failure statistics discussed in Section 3.2, where three modules fail the dry 40 MΩ·m^2 criterion and eight modules fail the IEC-wet criterion, with five modules showing dry-pass/wet-fail behavior.

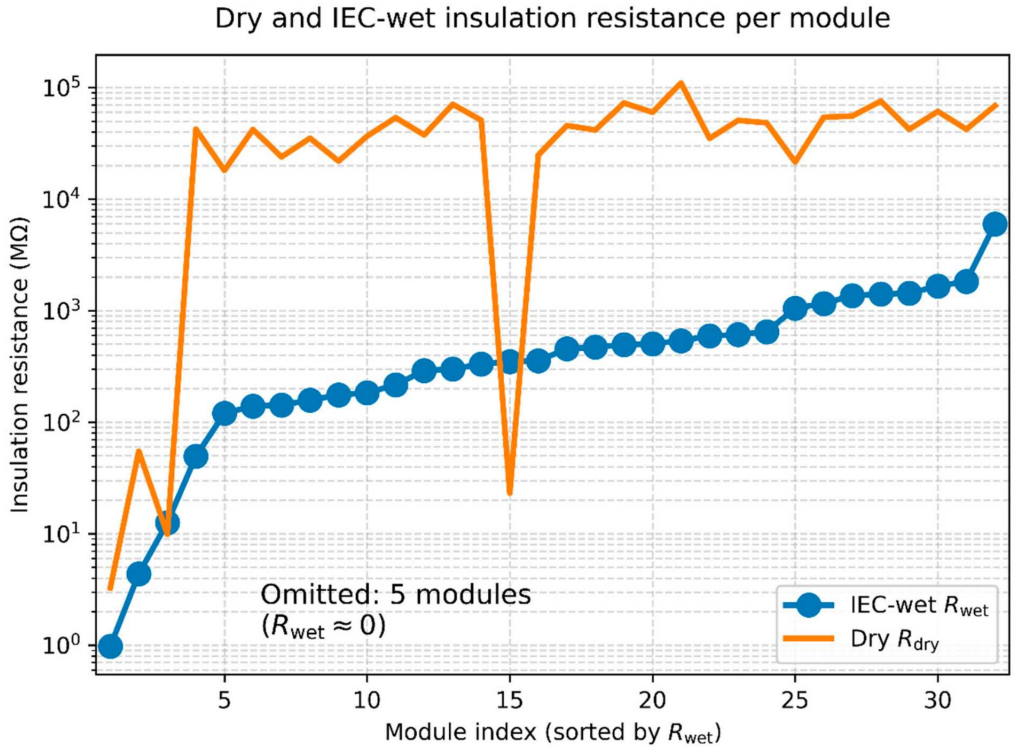

Figure 3. Dry (R_{dry}) and IEC-wet (R_{wet}) insulation resistances of the field-aged modules (log scale).

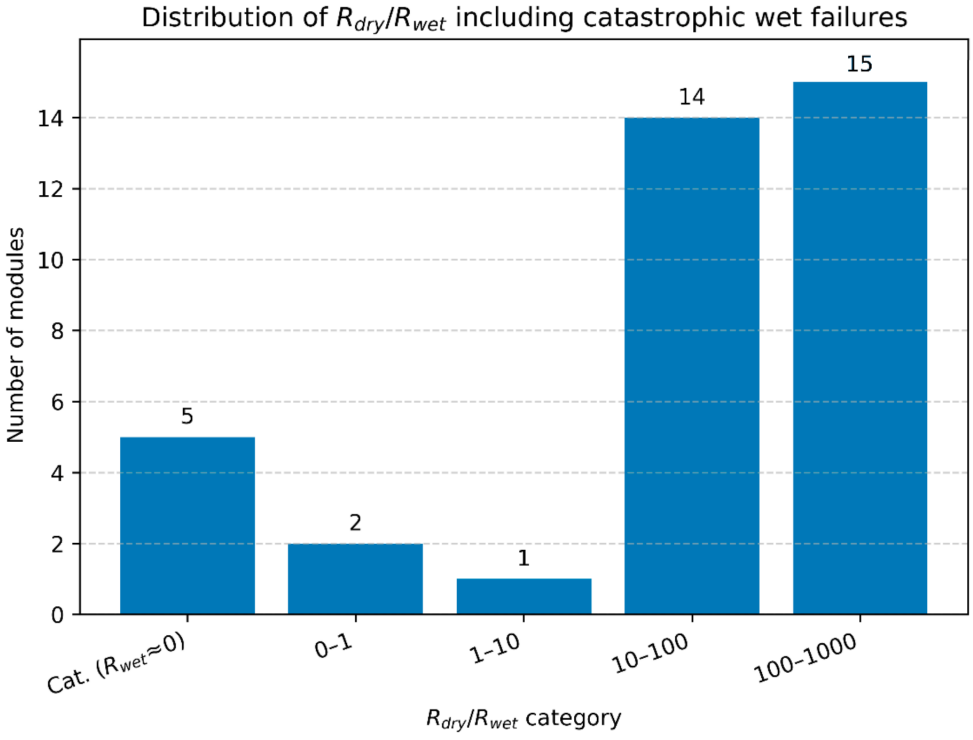

Figure 4. Distribution of the dry-to-wet insulation resistance ratio R_{dry}/R_{wet}, including catastrophic wet failure ("Cat.", R_{wet} = 0 Ω).

3.2. Compliance with the IEC 40 MΩ·m² Criterion and Dry-Pass/Wet-Fail Cases

For typical module areas A = 1.6, 1.8 and 2.0 m^2, the 40 MΩ·m^2 criterion translates into wet-resistance limits of 25.0 MΩ, 22.2 MΩ and 20.0 MΩ, respectively. Using A = 1.8 m^2 as an example, our dataset yields

- IEC-wet-pass modules: 29 modules;
- IEC-wet-fail modules: 8 modules (21.6% of the set);
- Dry-fail modules: 3 modules already below 22.2 MΩ in the dry state;
- Dry-pass/wet-fail modules: 5 modules that meet the dry criterion but fail the IEC-wet limit.

The summary statistics are listed in Table 2, and the IEC-wet pass/fail statistics are given in Table 3.

Table 2. Summary statistics for dry and IEC-wet insulation resistance and dry-to-wet ratio (N = 37).

Metric	R_{dry}	R_{wet}	Ratio R_{dry}/R_{wet}
Median	42.4 GΩ	462.5 MΩ	109.7×
Mean	(not used; skewed)	(not used; skewed)	543.5×
Minimum (non-zero)	3.27 MΩ (Panel 14)	4.38 MΩ (Panel 34)	0.07× (Panel 33)
Maximum	110.4 GΩ (Panel 15)	5.99 GΩ (Panel 7)	856.6× (Panel 12)

Table 3. Compliance of the 37 field-aged modules with the IEC 40 MΩ·m^2 insulation-resistance criterion for typical module areas.

Assumed Area A [m^2]	Wet Limit R_{limit} = 40/A [MΩ]	IEC Wet Pass [Count]	IEC Wet Fail [Count]	Dry Fail [Count]	Dry-Pass/Wet-Fail [Count]
1.6	25.0	29	8	4	5
1.8	22.2	29	8	3	5
2.0	20.0	29	8	3	5

Thus, relying on dry insulation resistance alone would have allowed 5 unsafe modules out of 37 (13.5%) to pass—the dry-pass/wet-fail population. In a large plant with tens of thousands of modules, this fraction could translate into hundreds of problematic units, with an increased risk of ground-fault trips and safety issues [3,5,6,12].

Figure 5 shows R_{dry} versus R_{wet} on logarithmic axes for modules with finite R_{wet}. Most modules lie above the diagonal $R_{dry} = R_{wet}$ confirming that $R_{dry} > R_{wet}$ typically holds. Two modules (Panels 10 and 33) lie below the diagonal $R_{dry} < R_{wet}$ The horizontal line indicates the IEC-wet limit $R_{wet} = 40/A$ for A = 1.8 m^2. The dry-pass/wet-fail modules have high R_{dry} values but lie below the IEC-wet limit, thus failing the wet criterion despite acceptable dry behavior.

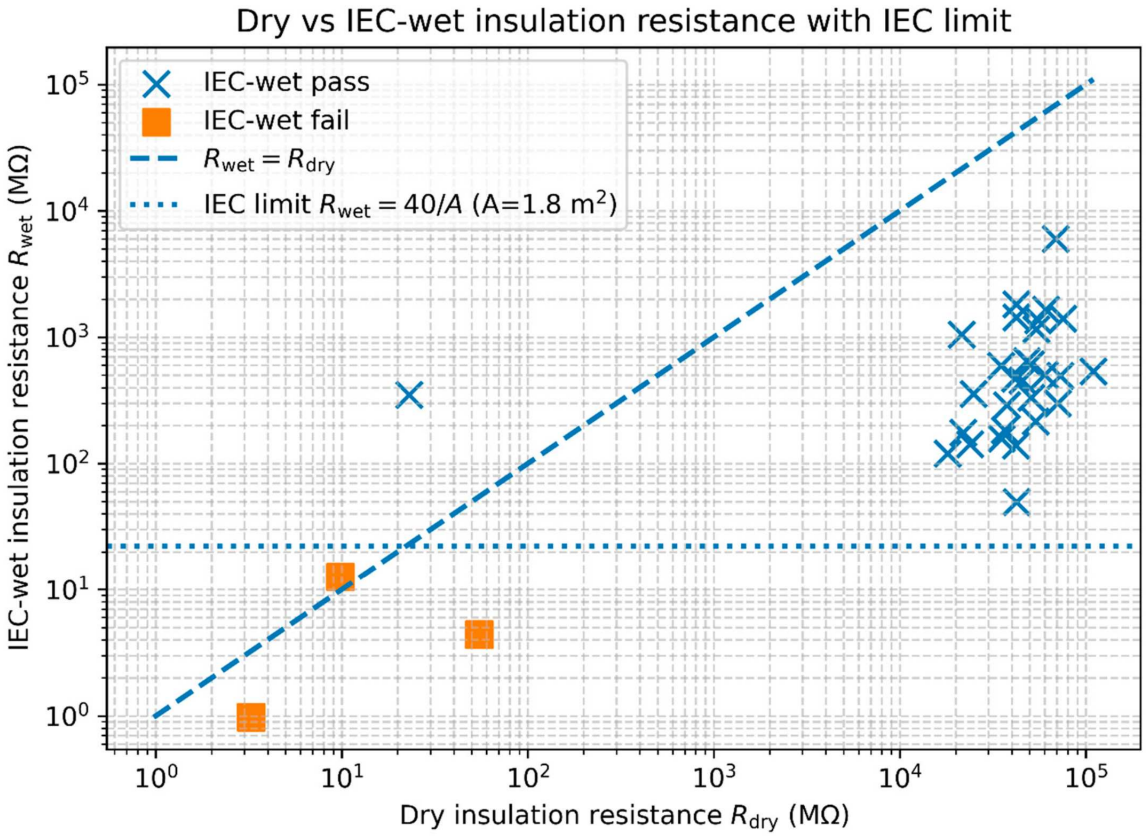

Figure 5. Scatter plot of dry insulation resistance Rdry versus IEC-wet resistance R_{wet} (log-log).

3.3. Practical Dry-Test Threshold

For A = 1.8 m^2, the modules were labeled IEC-wet-fail if $R_{wet} \times A$ < 40 MΩ·m^2. On the basis of this classification, we scanned candidate dry thresholds T and flagged modules with $R_{dry} < T$ as "at risk". For each threshold, we computed sensitivity and specificity as defined in Equations (3) and (4).

Figure 6 shows the sensitivity and specificity versus T on a logarithmic x-axis, together with a vertical line at T ≈ 55.5 GΩ (55 500 MΩ). As T increases from low values, the sensitivity rapidly approaches unity, meaning that virtually all the IEC-wet-failing modules are captured as at risk. Moreover, the specificity decreases because an increasing fraction of IEC-wet-passing modules is also flagged.

At $T \approx$ 55.5 GΩ, the sensitivity in our dataset is high (six of eight IEC-wet-failing modules are correctly flagged), whereas the specificity is low (only a minority of IEC-wet-passing modules correctly not flagged). This threshold is therefore deliberately conservative: it minimizes the likelihood of missing an IEC-wet failure at the expense of flagging many IEC-wet-passing modules. It is best understood as a triage indicator for prioritizing modules for IEC-wet verification rather than as a stand-alone pass/fail criterion.

To scale the threshold to other module sizes, a practical first-order area scaling consistent with the IEC area-normalized criterion is calculated using Equation (5):

$$T(A) = T_0 \cdot \frac{A_0}{A} \tag{5}$$

where T_0 = 55.5 GΩ was derived for A_0 = 1.8 m^2. Climate-specific calibration can be performed by wet-testing a representative subset from the most humidity-/dew-prone sites and adjusting T to the desired sensitivity level for that fleet.

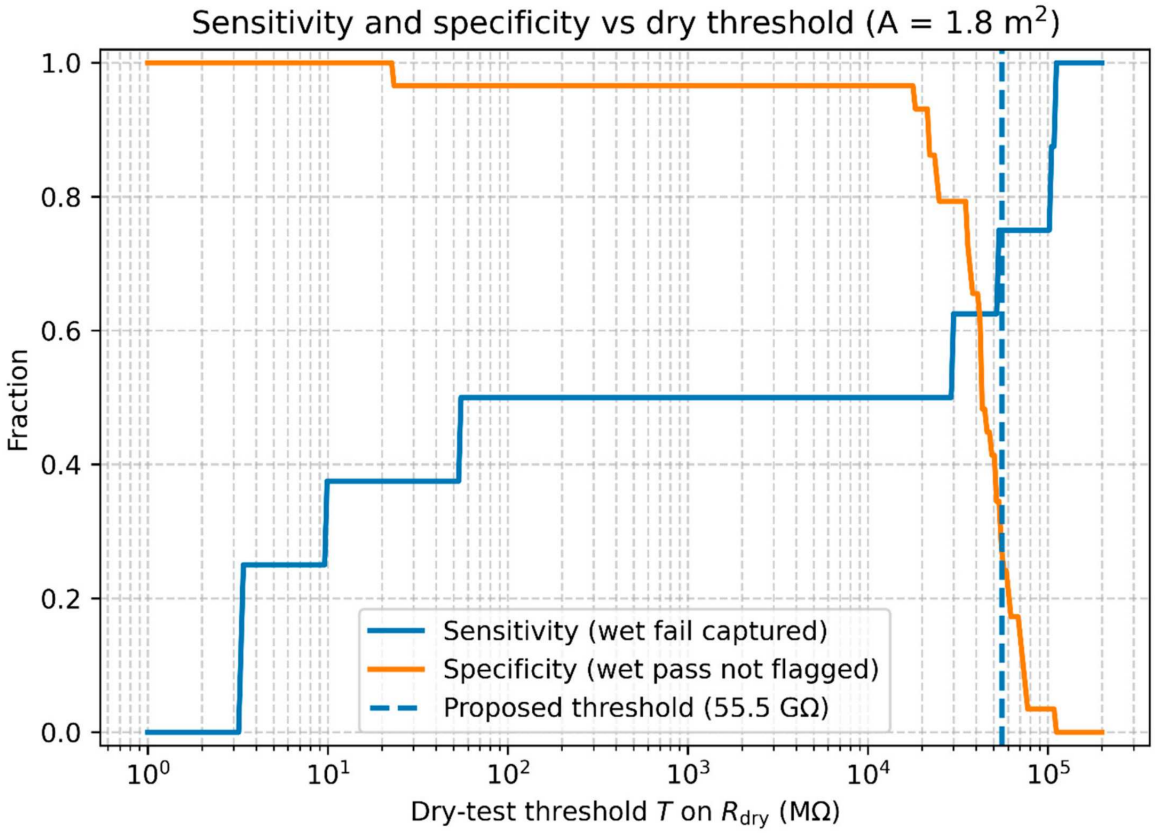

Figure 6. Sensitivity and specificity of IEC-wet failure prediction as a function of the dry-test threshold T on Rdry (assuming A = 1.8 m^2).

4. Discussion

4.1. Dew, Wet Conditions and Leakage Mechanisms

The strong dry-to-wet drop in R_{isol} observed in this work is consistent with the physical and electrochemical understanding of wet leakage in PV modules [3–6]. Glass-covered modules with high infrared emissivity radiate thermal energy to the night sky and can cool below the ambient temperature and the dew point, causing dew to form readily on the front glass, at frame edges and at mounting interfaces. Even in arid coastal deserts, elevated humidity can aggravate surface conductivity. Outdoor measurements in Jubail (Saudi Arabia) reported that relative humidity above 60% increased PV efficiency losses due to increased dust adhesion and moisture-induced conductive paths [24]. Thin water films and droplets create additional conductive pathways, lower surface resistivity, facilitate ionic transport into microcracks and degrade backsheets. Backsheet fragmentation after weathering exposure has been reported previously [25]. In combination with pre-existing material degradation, such moisture-assisted pathways can reduce insulation resistance by several orders of magnitude compared with dry conditions. Our measurements confirm this behavior: dry measurements overestimate wet insulation resistance by roughly two orders of magnitude at the median, and in several cases, wet failures are catastrophic ($R_{wet} \approx 0\ \Omega$).

The Namib beetle is used here only as an analogy: dew formation is a routine morning phenomenon in many climates, including temperate regions, and is therefore relevant well beyond deserts. This useful analogy is provided by the Namib desert beetle, whose elytra combine high infrared emissivity with a micro-textured surface [26] that promotes preferential condensation in the valleys between bumps. Figure 7 [27] schematically illustrates this "valley condensation" mechanism. In a similar way, dew on PV modules

tends to accumulate in regions with favorable micro-geometry and thermal coupling—such as frame edges, cell cut-outs and backsheet irregularities—forming localized water films and droplets that effectively shorten leakage paths to grounded metal parts and promote electrochemical reactions in polymeric components, thereby accelerating long-term degradation.

Figure 7. Schematic illustration of dew condensation on the elytra of the Namib desert beetle. Owing to its high infrared emissivity and surface micro-texture, dew preferentially forms in the valleys between bumps (photo credit: Solvin Zankl) [27].

From a system perspective, the most critical combination of conditions typically occurs around sunrise. After a long, humid night, modules often exhibit their highest surface moisture and thus their lowest insulation resistance, while at the same time, the module and cell temperatures are at their minimum, and the open-circuit voltage of the DC system is near its daily maximum. Consequently, many insulation-resistance alarms and ground-fault trips in operating plants are observed shortly after sunrise rather than at midday, when modules are warmer and partially dry [2–5,10,24]. Taken together, these considerations emphasize that wet insulation resistance is not an exceptional or extreme state but rather a regular operating condition during many mornings of the year across a wide range of climates, including a hot desert climate. IEC-conformant wet testing therefore mirrors real-world conditions far more closely than dry testing alone does and provides information directly relevant for safety assessments, O&M strategies and repowering decisions at the system level.

Pragmatic Leakage-Behavior Classes (Framework for Repowering/O&M)

To support practical O&M screening and repowering/revamping decisions, we propose a pragmatic classification of moisture-related leakage behavior based on the electrical signatures observed in this dataset ($N = 37$). The objective is not to claim a unique root cause for each module without destructive analysis, but to translate dry and IEC-wet insulation measurements into actionable decision categories. In particular, we distinguish catastrophic wet failures ($R_{wet} \approx 0\ \Omega$), non-catastrophic IEC-wet failures ($R_{wet} \cdot A < 40\ \mathrm{M\Omega \cdot m^2}$), and the critical dry-pass/wet-fail population, for which dry-only screening would miss IEC-wet non-compliance. Table 4 summarizes the proposed classes, their electrical signatures, indicative moisture-related leakage pathways consistent with prior reports on field-aged modules and backsheet-related insulation issues, and recommended practical actions. The

class boundaries for "high drop but wet pass" are intentionally defined as fleet-tunable (e.g., using a ratio threshold such as $R_{ratio} \geq 100$) to support risk-based sampling strategies.

Table 4. Proposed moisture-related leakage behavior classes and practical actions for O&M and repowering/revamping.

Class	Electrical Signature (Measured/Derived)	Indicative Moisture-Related Leakage Pathway (Examples; Non-Exhaustive)	Simple Inspection Indicator (Examples)	Recommended Action (O&M/Repowering)
C0 (Catastrophic wet failure)	$R_{wet} \approx 0\ \Omega$ (below instrument range); IEC-wet fail by definition	Severe moisture ingress and/or direct wet conduction (e.g., junction box seal/cable-gland ingress; severe insulation breakdown; water film shorting to frame)	Water inside junction box; damaged seals/grommets; visible corrosion/burn marks; severe backsheet cracking or delamination	Immediate isolation/mitigation; prioritize replacement; route removed modules to appropriate end-of-life handling
C1 (Wet fail, finite Rwet)	$R_{wet} \cdot A < 40\ M\Omega \cdot m^2$ (i.e., $R_{wet} < 40/A$); R_{wet} finite but below IEC limit	Strong moisture-assisted leakage under wetting (surface/edge conduction; moisture-assisted polymer/interface pathways; ageing-related backsheet/encapsulant degradation)	Cracked/embrittled backsheet; edge-seal degradation; delamination signs; corrosion at frame/ground points	Prioritize replacement during repowering/revamping; targeted inspection; consider batch-level screening
C2 (Dry-pass/wet-fail)	$R_{dry} \cdot A \geq 40\ M\Omega \cdot m^2$ AND $R_{wet} \cdot A < 40\ M\Omega \cdot m^2$ (dry passes, wet fails)	Wet-only leakage pathway dominates compliance (latent defect activated by wetting; localized surface conduction; moisture pathway not expressed in dry state)	Often visually subtle; may correlate with dew-/rain-sensitive alarms in the field	Do not rely on dry-only acceptance; prioritize IEC-wet verification and monitoring; replace if recurring or clustered
C3 (Wet pass, high drop/susceptible)	$R_{wet} \cdot A \geq 40\ M\Omega \cdot m^2$ AND Rratio = R_{dry}/R_{wet} is very large (e.g., ≥ 100; fleet-tunable)	Developing moisture-sensitive pathway (early-stage backsheet aging; edge conduction under wetting; contamination-assisted water film conduction)	Early backsheet whitening/crazing; mild edge changes; frequent dew-related insulation fluctuations	Increase wet-test sampling frequency; preventive inspection; consider earlier replacement if trend worsens
C4 (Wet pass, moderate drop/typical)	$R_{wet} \cdot A \geq 40\ M\Omega \cdot m^2$ AND Rratio moderate (e.g., 1–100; fleet-tunable)	Typical wetting response without evidence of critical defect	No specific indicator	Standard operation; routine sampling only

In practice, Classes C0–C2 should be prioritized for immediate action because they either represent catastrophic wet behavior or IEC-wet non-compliance, including cases that dry tests can miss. Classes C3–C4 can support fleet management by identifying modules that are susceptible (large dry-to-wet drop) versus those showing typical behavior, thereby helping to allocate IEC-wet testing capacity to the most informative subsets of a large PV fleet).

4.2. Implications for Testing Strategies of Field-Aged Modules

At present, IEC 61215 MQT 15 is mainly applied for type approval of new products, whereas field-aged modules in operating plants and secondary markets are rarely subjected to IEC-conformant wet testing. Here, we address this gap by applying MQT 15 to $N = 37$ field-aged modules and quantifying dry-pass/wet-fail cases against the IEC 40 $M\Omega \cdot m^2$ criterion, which is consistent with morning-dew wetting as a common

real-world condition [1,2,7,23]. Our results suggest several practical implications for testing strategies.

First, dry-only testing is insufficient to guarantee safety. In this moderate dataset, three modules (8.1%) already fail the IEC criterion in the dry state, but eight modules (21.6%) fail under IEC-wet conditions, including five dry-pass/wet-fail cases. In utility-scale plants, similar fractions correspond to many hundreds of problematic modules and could lead to nuisance trips or safety incidents [2–6,10,12].

Second, IEC-wet testing should be considered for field-aged modules, at least on a sampling basis, in climates with frequent dew or heavy precipitation, in hot desert climates with morning dew and in plants where backsheet-driven insulation issues are suspected [4–10]. IEC-wet tests capture leakage paths that only form under wet operation and reveal catastrophic failures that dry tests miss.

Third, the proposed dry threshold of ≈55.5 GΩ (for A = 1.8 m^2) can be used as a conservative screening indicator: modules with R_{dry} values below this threshold are prioritized for IEC-wet verification and detailed inspection, whereas modules with higher R_{dry} values are lower priority. Thresholds can be adapted to fleet-specific data, risk tolerance and available testing capacity, with first-order scaling via Equation (5).

Fourth, for new plants, operators may consider incorporating insulation-resistance monitoring and periodic wet testing into their operation and maintenance strategies, especially for module designs and backsheet materials known to show strong wet-resistance degradation [4,6–8].

In summary, integrating IEC-type wet testing into the toolkit for field-aged modules can significantly improve the robustness of safety assessments while still using dry measurements as a fast first-line screening tool. The key quantitative message is the contrast between three dry failures and eight wet failures, including five dry-pass/wet-fail modules, in what might otherwise appear to be a healthy population.

4.3. Repowering/Revamping Decisions and End-of-Life Management

In high-irradiance regions with very low PV LCOE, partial repowering/revamping—replacing older modules with newer technology after 5–10 years—can be economically attractive [18–22]. Case studies of premature field failure have shown that the effective service life can be limited to only 3–6 years for some material combinations because of issues such as potential-induced degradation (PID) [28], delamination, moisture ingress or early-generation polyamide backsheets [6–8,19,20]. In these situations, early module replacement in a repowering strategy can restore plant performance and extend system lifetime.

The wet insulation resistance provides an additional decision parameter in this context:

- Modules that pass both dry and IEC-wet tests and show acceptable power output can be kept in service until performance degradation or mechanical wear justifies replacement;
- Modules that fail the IEC-wet criterion or exhibit catastrophic wet behavior ($R_{wet} \approx 0\ \Omega$) represent a safety and reliability risk, even if their dry resistance remains high; these modules should be prioritized for replacement during repowering campaigns;
- By combining dry thresholds (e.g., 55.5 GΩ) with IEC-wet tests, operators can identify sub-arrays or module batches that merit priority replacement versus those that can be retained or redeployed in less demanding applications (e.g., low-voltage systems with enhanced protection).

From a sustainability perspective, repowering/revamping decisions and end-of-life management are tightly linked. Modules removed for safety reasons or as part of repowering campaigns can be directed to advanced and sustainable recycling processes, supporting circular-economy objectives while reducing environmental impact [11,14–17]. In sunny and

hot climates with annual specific yields of up to approximately 1800 kWh/kW, the return on investment (ROI) can be shorter than five years [18–20]. In such contexts, repowering or revamping within 5–10 years can be economically feasible, and reliable wet-insulation-resistance data help ensure that sustainability considerations are fully integrated into technical and financial decision-making.

Manufacturing Constraint (Figure 8; Requested Addition)

Short repowering intervals imply that PV module manufacturing capacity can become increasingly allocated to replacements rather than new deployments. For example, for a PV module factory with a production capacity of 1 GW/year, a 5-year repowering interval means that after the first 5 years the factory output is assumed to be fully consumed by replacing modules from the already-installed fleet, leaving no production capacity for new PV power plants (Figure 8). This is a conceptual illustration assuming full replacement at the stated interval.

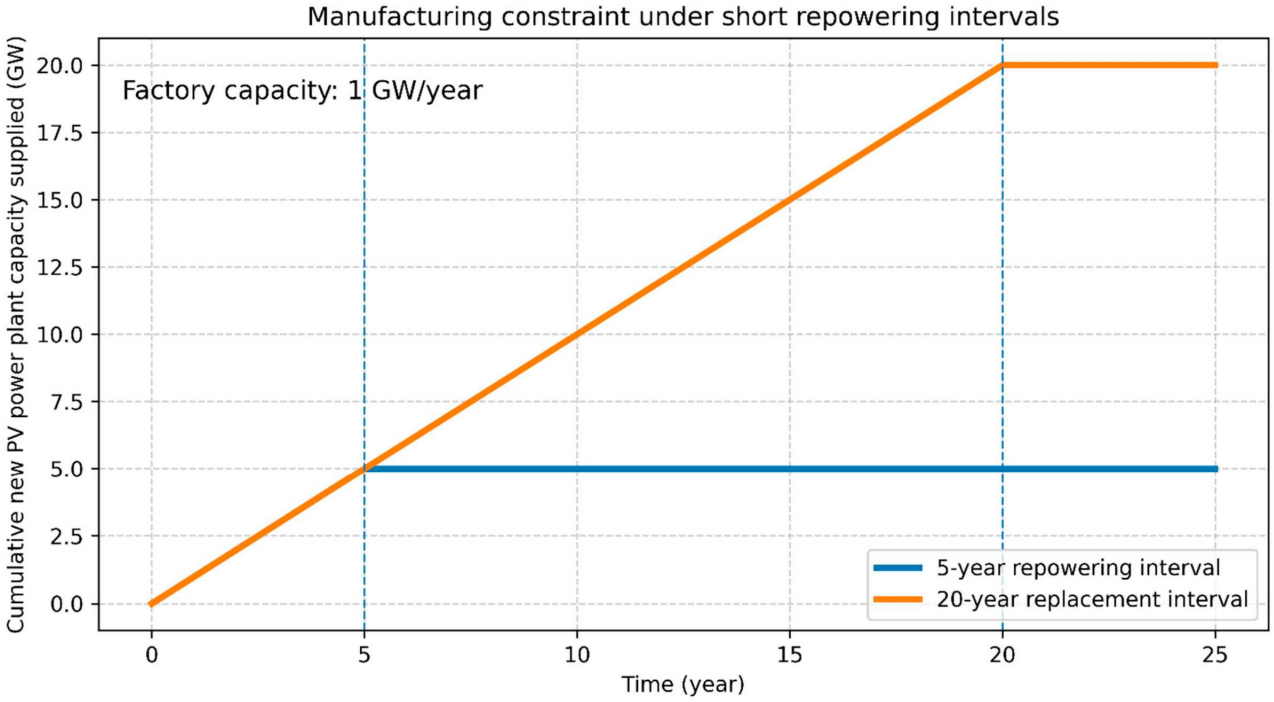

Figure 8. Illustration of the manufacturing constraint for a PV panel factory with a production capacity of 1 GW/year.

The curves show the cumulative new PV power plant capacity that can be supplied by the factory before its output is fully consumed by replacement (repowering) demand. With a 5-year repowering interval, the factory can supply approximately 5 GW of new PV capacity in the first 5 years (1 GW/year × 5 years); after year 5, production is assumed to be used only for replacing faulty/repowered panels in the existing fleet, leaving no further capacity for new PV power plants (plateau at ~5 GW). For comparison, with a 20-year replacement interval, the same factory could supply ~20 GW of new PV capacity before its output would be fully consumed by replacement demand (plateau at ~20 GW). This is a conceptual illustration assuming full replacement at the stated interval.

4.4. Potential Drawbacks and Unintended Consequences of Stricter Wet-Condition Requirements

Strengthening wet-condition requirements (or extending IEC-conformant wet testing to field-aged and second-life modules) could improve safety screening, but several practical drawbacks and unintended consequences should be considered [1,7,23]. First, IEC-style wet

testing is more time- and infrastructure-intensive than dry insulation screening, which can limit adoption in routine O&M and secondary-market workflows. Second, stricter thresholds can increase false alarms in fleets where wetting conditions are rare or where protection architecture reduces risk, potentially leading to premature replacements and additional embodied impacts [14–17]. Third, wet-test outcomes depend on boundary conditions (solution conductivity, wetting of junction box/cables, dwell time, temperature) defined by the standard and related procedural guidance; therefore, tighter requirements should be paired with clear reproducibility and comparability guidance [1,23]. Finally, design pressure to "pass wet tests" may shift material choices (backsheets, sealants) with trade-offs for cost, recyclability, and long-term aging modes that have been observed to differ across backsheet families [5,8–10,25]. Therefore, a risk-based approach is recommended: dry tests as rapid triage combined with targeted IEC-wet verification and mechanism-informed inspection in suspect subpopulations [1,7].

5. Conclusions

We measured the dry and IEC-wet insulation resistance of 37 field-aged crystalline-silicon PV modules and used these data to evaluate the adequacy of dry-only testing and to explore implications for repowering/revamping and sustainable PV deployment and asset management. A key novelty of this work is the direct comparison of dry and wet ground impedance tests to a statistically meaningful set of field-aged PV modules (N = 37) and the interpretation of dry-pass/wet-fail behavior in the context of routine morning-dew wetting [1,2,7,23]. The main conclusions are as follows:

1. Dry measurements can strongly overestimate wet insulation resistance. The median ratio R_{dry}/R_{wet} is $\approx 110\times$, with a long high-ratio tail where some modules show drops of more than two orders of magnitude, and several modules exhibit catastrophic wet behavior with $R_{wet} \approx 0\ \Omega$ [3,6,12].

2. Dry-only testing can miss wet-insulation failures. In this dataset, three modules fail the IEC 40 M$\Omega \cdot$m^2 criterion in the dry state, whereas eight modules fail under IEC-wet conditions. Five of the wet-failing modules are dry-pass/wet-fail cases, demonstrating that dry-only testing is not sufficient to ensure compliance under wet operation [1,3–7].

3. A conservative dry-test threshold of approximately 55.5 GΩ (for A = 1.8 m^2) provides high sensitivity but low specificity for predicting IEC-wet failure. This threshold is best used as a triage indicator to prioritize modules for IEC-wet verification and closer inspection rather than as a stand-alone acceptance criterion within a testing and risk-management strategy. First-order scaling to other module sizes is possible via $T(A) \propto 1/A$.

4. IEC-conformant wet testing of field-aged modules—at least on a sampling basis—should be considered in climates with frequent dew or heavy precipitation, in hot desert climates with morning dew and where backsheet-related insulation problems are suspected [2–8] as part of sustainable operation and maintenance practices.

5. Wet insulation resistance is highly relevant for the end-of-life decisions of PV panels and for repowering/revamping within 5–10 years, particularly in demanding hot climates. It helps identify modules that should be removed for safety reasons during repowering campaigns and directed to appropriate recycling routes [11,14–17], thereby aligning operational safety with a circular-economy and sustainability objectives.

The incorporation of wet insulation testing into the standard assessment of used and field-aged PV modules is therefore recommended as a practical step toward safer, more reliable and more sustainable PV deployment.

Author Contributions: Conceptualization, V.P.; methodology, V.P. and V.B.; investigation, V.P., V.B. and M.K.; formal analysis, T.F.; writing—original draft preparation, V.P. and T.F.; writing—review and editing, all authors. All authors have read and agreed to the published version of the manuscript.

Funding: This research received no external funding.

Institutional Review Board Statement: Not applicable.

Informed Consent Statement: Not applicable.

Data Availability Statement: The cleaned dataset of dry and wet insulation resistance values, together with analysis scripts, is available from the corresponding author upon reasonable request.

Conflicts of Interest: The authors declare no conflicts of interest.

References

1. *IEC 61215-2:2021*; Terrestrial Photovoltaic (PV) Modules—Design Qualification and Type Approval—Part 2: Test Procedures (MQT 15: Wet Leakage Current Test). International Electrotechnical Commission: Geneva, Switzerland, 2021. Available online: https://webstore.iec.ch/en/publication/61350 (accessed on 7 December 2025).
2. Simsek, E.; Williams, M.J.; Pilon, L. Effect of dew and rain on photovoltaic solar cell performances. *Sol. Energy Mater. Sol. Cells* **2021**, *222*, 110908. [CrossRef]
3. Hernández, J.; Vidal, P.; Medina, A. Characterization of the insulation and leakage currents of PV generators: Relevance for human safety. *Renew. Energy* **2010**, *35*, 593–601. [CrossRef]
4. Roy, J.N. Modelling of insulation characteristics of Solar Photovoltaic (SPV) modules. *Sol. Energy* **2015**, *120*, 1–8. [CrossRef]
5. Buerhop, C.; Stroyuk, O.; Zöcklein, J.; Pickel, T.; Hauch, J.; Peters, I.M. Wet Leakage Resistance Development of Modules with Various Backsheet Types. *Prog. Photovolt. Res. Appl.* **2022**, *30*, 938–947. [CrossRef]
6. Ketjoy, N.; Mensin, P.; Chamsa-Ard, W. Impacts on insulation resistance of thin film modules: A case study of a flooding of a photovoltaic power plant in Thailand. *PLoS ONE* **2022**, *17*, e0274839. [CrossRef]
7. Anagha, E.; Kulkarni, S.; Shiradkar, N. Development of a characterization technique to effectively detect latent insulation defects in the field-deployed PV modules. *Sol. Energy Mater. Sol. Cells* **2025**, *292*, 113761. [CrossRef]
8. Buerhop-Lutz, C.; Stroyuk, O.; Pickel, T.; Winkler, T.; Hauch, J.; Peters, I.M. PV modules and their backsheets—A case study of a Multi-MW PV power station. *Sol. Energy Mater. Sol. Cells* **2021**, *231*, 111295. [CrossRef]
9. Lutz, C.B.; Lüer, L.; Stroyuk, O.; Hauch, J.; Peters, I.M. Dynamics of backsheet-driven insulation issues. *Sol. Energy Mater. Sol. Cells* **2023**, *257*, 112398. [CrossRef]
10. Stroyuk, O.; Güttler, C.; Buerhop-Lutz, C.; Hauch, J.; Peters, I.M. Identification of the Backsheet Type of Silicon Photovoltaic Modules from Encapsulant Fluorescence Images. *ACS Appl. Energy Mater.* **2023**, *6*, 2340–2346. [CrossRef]
11. Poulek, V.; Beranek, V.; Kozelka, M.; Finsterle, T. Environmentally Sustainable Recycling of Photovoltaic Panels Laminated with Soft Polysiloxane Gels: Promoting the Circular Economy and Reducing the Carbon Footprint. *Sustainability* **2025**, *17*, 8167. [CrossRef]
12. Poulek, V.; Safrankova, J.; Cerna, L.; Libra, M.; Beranek, V.; Finsterle, T.; Hrzina, P. PV Panel and PV Inverter Damages Caused by Combination of Edge Delamination, Water Penetration, and High String Voltage in Moderate Climate. *IEEE J. Photovolt.* **2021**, *11*, 561–565. [CrossRef]
13. Finsterle, T.; Kasper, J.; Hrzina, P.; Knap, V.; Černá, L. The Effect of Backsheet Repairs on Insulation Resistance in Photovoltaic Modules. *Monatshefte Chem.* **2025**, *156*, 559–567. [CrossRef]
14. Papamichael, I.; Voukkali, I.; Jeguirim, M.; Argirusis, N.; Jellali, S.; Sourkouni, G.; Argirusis, C.; Zorpas, A.A. End of Life Management and Recycling on PV Solar Energy Production. *Energies* **2022**, *15*, 6430. [CrossRef]
15. Gerold, E.; Antrekowitsch, H. Advancements and Challenges in Photovoltaic Cell Recycling: A Comprehensive Review. *Sustainability* **2024**, *16*, 2542. [CrossRef]
16. Akhter, M.; Al Mansur, A.; Islam, M.I.; Lipu, M.H.; Karim, T.F.; Abdolrasol, M.G.; Alghamdi, T.A. Sustainable Strategies for Crystalline Solar Cell Recycling: A Review on Recycling Techniques, Companies, and Environmental Impact Analysis. *Sustainability* **2024**, *16*, 5785. [CrossRef]
17. Królicka, A.; Maj, A.; Łój, G. Promoting Sustainability in the Recycling of End-of-Life Photovoltaic Panels and Li-Ion Batteries Through LIBS-Assisted Waste Sorting. *Sustainability* **2025**, *17*, 838. [CrossRef]
18. IEA PVPS. *Trends in Photovoltaic Applications 2025*; International Energy Agency Photovoltaic Power Systems Programme: Paris, France, 2025; Available online: https://iea-pvps.org/wp-content/uploads/2025/10/IEA-PVPS_Trends_2025-.pdf (accessed on 7 December 2025).
19. IRENA. *Renewable Power Generation Costs in 2020*; International Renewable Energy Agency: Abu Dhabi, United Arab Emirates, 2021.
20. Fraunhofer ISE. *Photovoltaics Report*; Fraunhofer Institute for Solar Energy Systems ISE: Freiburg, Germany, 2025. Available online: https://www.ise.fraunhofer.de/en/publications/studies/photovoltaics-report.html (accessed on 7 December 2025).
21. Villena-Ruiz, R.; Martín-Martínez, S.; Honrubia-Escribano, A.; Ramírez, F.J.; Gómez-Lázaro, E. Solar PV power plant revamping: Technical and economic analysis of different alternatives for a Spanish case. *J. Clean. Prod.* **2024**, *446*, 141439. [CrossRef]

22. Jean, J.; Woodhouse, M.; Bulović, V. Accelerating Photovoltaic Market Entry with Module Replacement. *Joule* **2019**, *3*, 2824–2841. [CrossRef]
23. Firman, A.; Cáceres, M.; González Mayans, A.R.; Vera, L.H. Photovoltaic Qualification and Approval Tests. *Standards* **2022**, *2*, 136–156. [CrossRef]
24. Almarri, A.; AlMutairi, R.; Alnass, F.; Alghamdi, N.; Ghobashy, M.M.; Attia, M.S.; Madani, M. Experimental and modeling study of dust composition impact on photovoltaic performance in arid coastal environments. *J. Mater. Res. Technol.* **2025**, *39*, 5455–5467. [CrossRef]
25. Kempe, M.D.; Lyu, Y.; Kim, J.H.; Felder, T.; Gu, X. Fragmentation of photovoltaic backsheets after accelerated weathering exposure. *Sol. Energy Mater. Sol. Cells* **2021**, *226*, 111044. [CrossRef]
26. Guadarrama-Cetina, J.; Mongruel, A.; Medici, M.G.; Baquero, E.; Parker, A.R.; Milimouk-Melnytchuk, I.; González-Viñas, W.; Beysens, D. Dew Condensation on Desert Beetle Skin. *Eur. Phys. J. E* **2014**, *37*, 109. [CrossRef] [PubMed]
27. Zankl, S. A Fog Basking Beetle (*Onymacris unguicularis*) on the Crest of a Sand Dune in the Namib Desert is Drinking Droplets of Water Which Gather on Its Body During the Early Morning Fog over the Dunes. PhotoShelter/Solvin Zankl. Available online: https://solvinzankl.photoshelter.com/image?&_bqG=148&_bqH=eJyLSA4JqDQqC_LJMYkvyw4089JNT_N2zCszT7awMjKzsDI0MABhIOkZ7xLsbJuXmJuZpAZmxzv6udiWANmhwa5B8Z4utqEgdS4GGT5lvsVJTm6BavGOziG2xamJRckZAGbLH1s-&GI_ID= (accessed on 7 December 2025).
28. Luo, W.; Khoo, Y.S.; Hacke, P.; Naumann, V.; Lausch, D.; Harvey, S.P.; Singh, J.P.; Chai, J.; Wang, Y.; Aberle, A.G.; et al. Potential-induced degradation in photovoltaic modules: A critical review. *Energy Environ. Sci.* **2017**, *10*, 43–68. [CrossRef]